Bull. Mater. Sci., Vol. 26, No. 5, August 2003, pp. 517–521. © Indian Academy of Sciences.

Structural and magnetic properties of $Co_{1+y}Sn_yFe_{2-2y-x}Cr_xO_4$ ferrite system

A A PANDIT, S S MORE, R G DORIK and K M JADHAV*

Department of Physics, Dr Babasaheb Ambedkar Marathwada University, Aurangabad 431 004, India

MS received 12 February 2001; revised 23 May 2003

Abstract. **The samples of the series $Co_{1+y}Sn_yFe_{2-2y-x}Cr_xO_4$ ferrites with $x = 0{\cdot}0$, $0{\cdot}1$, $0{\cdot}2$, $0{\cdot}3$, $0{\cdot}4$, $0{\cdot}5$ and $y = 0{\cdot}05$, were prepared by the usual double sintering ceramic technique. The single-phase spinel structure of the samples was confirmed by using X-ray diffractometry technique. The lattice parameter '*a*' with an accuracy of $\pm 0{\cdot}002$ Å were determined using Bragg peaks of XRD pattern. The lattice parameter '*a*' decreases with concentration, *x*, which is due to the difference in the ionic radii of Cr^{3+} and Fe^{3+} ions. The X-ray intensity calculations were carried out in order to determine the possible cation distribution amongst tetrahedral (A) and octahedral [B] sites. The X-ray intensity calculations show Cr^{3+} ions occupying B site. The saturation magnetization, s_s, and magneton number, n_B (the saturation magnetization per formula unit), measured at 300 K determined from high field hysteresis loop technique decrease with increase in concentration, *x*, suggesting a decrease in ferrimagnetic behaviour. Thermal variation of low field a.c. susceptibility measurements from room temperature to about 800 K exhibits almost normal ferrimagnetic behaviour and the Curie temperature, T_C determined from a.c. susceptibility data decreases with increase in *x*.**

Keywords. **Spinel ferrite; cation distribution; magnetization; a.c. susceptibility; Curie temperature.**

1. Introduction

Spinel ferrites are technologically important class of magnetic oxides because of their magnetic properties, high electrical resistivity, low eddy current and dielectric loss. Ferrites are extensively used in microwave devices, computers, memory chips, magnetic recording media etc. Knowledge of cation distribution and spin alignment is essential to understand the magnetic properties of spinel ferrites. The interesting physical and chemical properties of ferro-spinels arise from their ability to distribute the cations among the available tetrahedral (A) and octahedral [B] sites (Blasse 1964). Cobalt ferrite possesses an inverse spinel structure and the degree of inversion depends upon heat treatment (Sawataky *et al* 1968).

It has been reported by many workers that the addition of tetravalent ions like Si^{4+}, Ge^{4+} and Ti^{4+} in cobalt ferrite influences the structural, electrical and magnetic properties (Shinde *et al* 1998; Nogues *et al* 1991; Joshi *et al* 1993). The substitution of Cr^{3+} ions is likely to increase the resistivity and decrease the saturation magnetization (Bradley 1971). The addition of tetravalent ions like Sn^{4+}, Ti^{4+} in spinel ferrite may also influence the electrical and magnetic properties. A smaller substitution of Sn^{4+} ions in ferrite may lead to increase in resistivity and segregating the grain boundaries and hence acts to decrease the dielectric properties. However, a large substitution of Sn^{4+} ion causes discontinuous grain growth to degenerate the magnetic property. Therefore, to see the effect of Cr^{3+} substitution in presence of small amount of Sn^{4+} in cobalt ferrite, the studies on $Co_{1+y}Sn_yFe_{2-2y-x}Cr_xO_4$ ferrites are undertaken.

No systematic investigations of the crystal structure, cation distribution and magnetic properties of $Co_{1+y}Sn_yFe_{2-2y-x}Cr_xO_4$ for $x = 0{\cdot}0$ to $0{\cdot}5$ and $y = 0{\cdot}05$ have been reported in the literature. The purpose of this paper is to report the results of our investigations of the crystal structure, cation distribution, saturation magnetization and Curie temperature of $Co_{1+y}Sn_yFe_{2-2y-x}Cr_xO_4$ (for $x = 0{\cdot}0$ to $0{\cdot}5$ and $y = 0{\cdot}05$) spinels by means of X-ray diffraction, magnetization and a.c. susceptibility measurements.

2. Experimental

Samples of the spinel series $Co_{1+y}Sn_yFe_{2-2y-x}Cr_xO_4$ for $x = 0{\cdot}0$, $0{\cdot}1$, $0{\cdot}2$, $0{\cdot}3$, $0{\cdot}4$ and $0{\cdot}5$, and $y = 0{\cdot}05$ were prepared by the usual double sintering ceramic method. The starting materials were Fe_2O_3, CoO, SnO_2 and Cr_2O_3 (99·9% pure) supplied by E. Merck. The oxides were mixed thoroughly in stoichiometric proportions to yield the desired composition and then wet ground. The mixture was dried and pressed into pellets. The pressure of 5 tons per square inch was applied on the pellet. These pellets were presintered at 900°C for 12 h and slowly cooled

*Author for correspondence

to room temperature. The samples were again powdered, pressed into pellets, sintered at 1100°C for 24 h and cooled slowly to room temperature at the rate of 2°C/min.

The X-ray patterns of all the samples were recorded at room temperature with a Philips (model PW 1710) diffractometer and the analysis of X-ray diffraction patterns proved that the studied samples have single phase cubic spinel structure. Magnetization measurements on each sample were carried out using the high field hysteresis loop technique (Radhakrishnamurty *et al* 1971) at 300 K. The a.c. susceptibility measurements on powdered samples were carried out in the temperature range 300–800 K using the double coil set-up (Radhakrishnamurty *et al* 1978).

3. Results and discussion

The single phase formation of the composition of the ferrite has been confirmed from X-ray diffraction pattern. Figure 1 depicts typical XRD patterns for $x = 0{\cdot}1$, $0{\cdot}2$ and $0{\cdot}5$. The lattice parameter 'a' determined from XRD data is shown in figure 2 as a function of x and same is listed in table 1. It can be seen from figure 2 that the lattice parameter 'a' initially increases up to $x = 0{\cdot}2$ and then decreases with x. The decrease in 'a' with x can be explained on the basis of difference in ionic radii of Fe^{3+} and Cr^{3+}. The smaller ionic crystal radius of Cr^{3+} (0·63 Å) replaces larger crystal radius Fe^{3+} (0·67 Å) which results in decreasing the lattice parameter 'a'. Nonlinear behaviour, on the other hand, is reported for systems which are not completely normal or inverse (Khan *et al* 1982). Accepting that ferrite is inverse, chromite is normal and the chromium ions always occupy octahedral [B] site, the change in 'a' with x indicates that cobalt ferrite chromite series changes structure from inverse to a certain degree of normal as x increases from 0·0 to 0·2 and approaches to a normal structure of cobalt chromite in the range $0{\cdot}2 < x < 0{\cdot}5$.

The X-ray density for each composition was calculated using the relation (Cullity 1959)

$$d_x = ZM/NV \text{ g/cm}^3, \tag{1}$$

where, Z is the number of molecules per unit cell ($Z = 8$), M the molecular weight, N the Avogadro's number and V the theoretical value of the unit cell volume. The X-ray density for each composition is summarized in table 1. It is evident from table 1 that X-ray density decreases up to $x = 0{\cdot}2$ and then increases, which is attributed to the variation of 'a' with x.

The XRD line width and particle size are connected through the Scherrer equation (Cullity 1959)

$$t = 0{\cdot}9\ l/B \cos q_B, \tag{2}$$

where, t is particle diameter, l the wavelength of the X-ray radiation, B a measure of the broadening of diffraction line due to size effect, B the full width at half maxima of the XRD line of the sample. The particle size estimated from Scherrer formula is summarized in table 1.

Using the experimental values of 'a' and oxygen positional parameter 'u' of each sample in the equation (Otero Arean *et al* 1990)

$$d_{Ax} = a\ 3(u - 1/4) \text{ tet bond}, \tag{a}$$

$$d_{Bx} = a(3u^2 - 11/4\ u + 43/64)^{1/2} \text{ oct bond}, \tag{b}$$

$$d_{Bx} = a\ 2(2u - 1/2) \text{ tet edge}, \tag{c}$$

$$d_{Xx} = a\ 2(1 - 2u) \text{ tet bond}, \tag{d}$$

$$d_{Xx} = a(4u^2 - 3u + 11/16)^{1/2} \text{ unshared oct edge}, \tag{e}$$

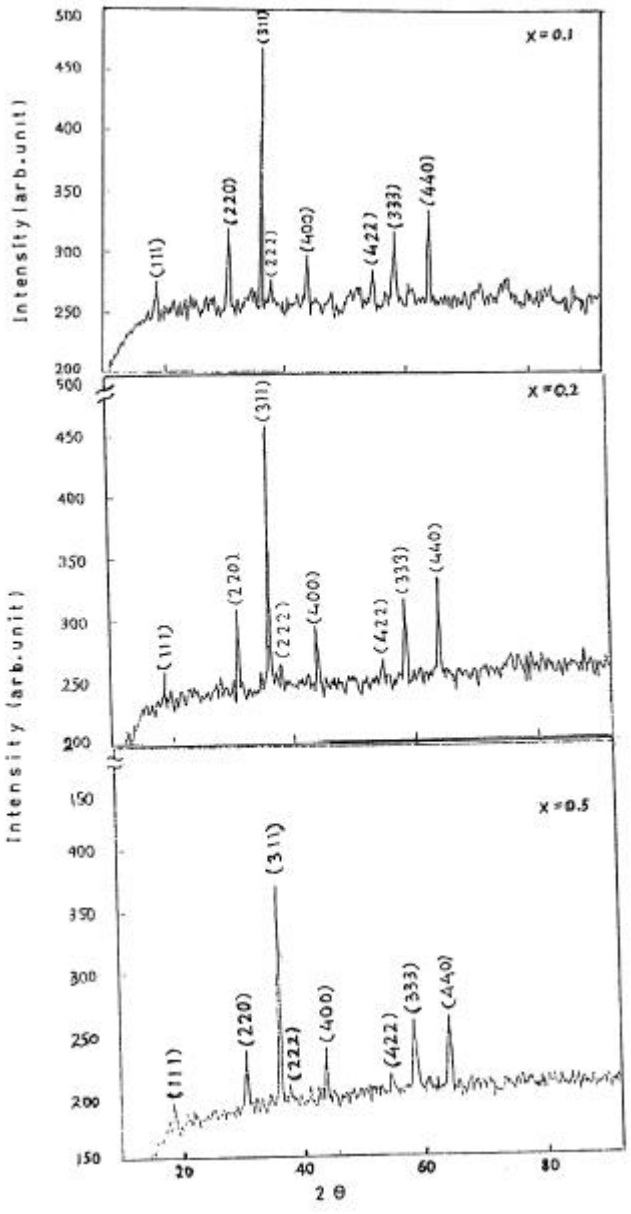

Figure 1. Typical XRD pattern for $Co_{1+y}Sn_yFe_{2-2y-x}Cr_xO_4$ system ($x = 0{\cdot}1$, $0{\cdot}2$, $0{\cdot}5$).

we calculate the selected interionic distances and the radius of the tetrahedral and octahedral interstices of all the samples from d_{Ax} and d_{Bx} and taking 1·32 Å as the radius of the divalent oxygen ions. Table 2 summarizes the values of oxygen positional parameter u, octa edge and radius of tetrahedral and octahedral interstices in $Co_{1+y}Sn_yFe_{2-2y-x}Cr_xO_4$. These values were calculated taking the value of oxygen positional parameter approximately equal to 0·375 for all the values of x.

Comparing the site preference energies of the constituent ions (Goodenough and Loeb 1953), the cation distribution of $Co_{1·05}Sn_{0·05}Fe_{1·9}O_4$ has been accepted as

$$(Co_{0·04}Fe_{0·96})^A[Sn_{0·05}Co_{1·01}Fe_{0·94}]^BO_4. \quad (3)$$

In order to determine the cation distribution, X-ray diffraction intensity calculations were carried out using the formula suggested by Buerger (1960),

$$I_{hkl} = |F_{hkl}|^2 P{\cdot}L_P, \quad (4)$$

where, notations have their usual meanings.

In accordance with the site preference energies, the Cr^{3+}, Sn^{4+} and Co^{2+} occupy B site, whereas the Fe^{3+} ions show no definite site preference (Goodenough and Loeb 1953).

The distribution of divalent, trivalent and tetravalent cation amongst octahedral and tetrahedral sites in the $Co_{1·05}Sn_{0·05}Fe_{1·9-x}Cr_xO_4$ was determined from the ratio of X-ray diffraction lines, $\boldsymbol{I}_{220}/\boldsymbol{I}_{440}$ and I_{400}/I_{440}. These ratios are considered to be sensitive to the cation distribution (Ohinishi and Teranishi 1961). The absorption and temperature factors are not taken into account in our calculations because these do not affect the relative intensity calculations for spinels at room temperature (Porta *et al* 1974). The formulae for the structure factors for the plane (*hkl*) are taken from those reported by Furuhashi *et al* (1973). The multiplicity and Lorentz polarization factors are taken from the literature (Otero Arean *et al* 1990). The cation distribution for which experimental ratios agree well with the observed intensity ratios is taken as correct one. The observed and calculated intensity ratio for the planes (220), (440), (400) are given in table 3.

Accepting the cation distribution of $Co_{1·05}Sn_{0·05}Fe_{1·9}O_4$ (3), the cation distribution for the $Co_{1+y}Sn_yFe_{2-2y-x}Cr_xO_4$ can be written as

$$(Fe_{0·96-0·4x}Co_{0·04+0·4x})\,[Fe_{0·94-0·6x}Sn_{0·05}Co_{1·01-0·4x}Cr_x].$$

X-ray intensity ratio calculation suggests that Cr^{3+} ions occupy octahedral B site. This is in good agreement with the results reported by Kwang *et al* (2000).

The saturation magnetization, s_s and the magnetization number, n_B (the saturation magnetization per formula unit in Bohr magneton), at 300 K obtained from the hysteresis loop technique for $x = 0·1$ to $0·5$ are summarized in table 4. It is evident from table 4 that all samples show ferrimagnetic behaviour which decrease with increase in x. The variation of n_B with x is shown in figure 3. The decrease in n_B with increased substitution of Cr^{3+} ions, shown in figure 3, can be explained on the basis of change in the magnetization, M_A and M_B, of tetrahedral (A) and octahedral [B] sublattices, respectively. Since Cr^{3+} ions occupy B sites more strongly as compared to both Fe^{3+} and Co^{2+} ions, the substitution of Cr^{3+} for Fe^{3+} in the present system leads to the migration of a small amount of Co^{2+} ions from B to A sites. The cation distribution obtained from X-ray diffraction and magnetization data is in good agreement and the same is represented in table 4.

According to Neel's (1950) two sub-lattice models of ferrimagnetism, the Neel's magnetic moment per formula unit in μ_B, n_B^N is expressed as

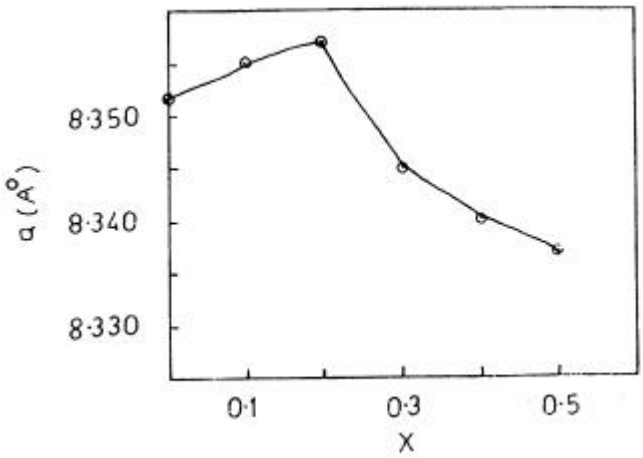

Figure 2. Variation of lattice constant '*a*' (Å) with Cr^{3+} concentration, *x*.

Table 1. Values of lattice constant, X-ray density and particle size for $Co_{1+y}Sn_yFe_{2-2y-x}Cr_xO_4$ ($y = 0·05$) system.

x	Lattice constant (Å)	Particle size (Å)	X-ray density (g/cm^3)
0·0	8·352	301	5·425
0·1	8·355	460	5·410
0·2	8·358	460	5·398
0·3	8·345	230	5·412
0·4	8·340	229	5·414
0·5	8·337	228	5·411

Table 2. Tet-edge, octa-edge, radius of tetrahedral and octahedral interstices.

		Octa-edge			
x	Tet-edge (Å)	Shared (Å)	Unshared (Å)	r_{tet} (Å)	r_{oct} (Å)
0·0	2·9528	2·9328	2·9528	1·8082	2·0880
0·1	2·9539	2·9539	2·9539	1·8089	2·0862
0·2	2·9546	2·9546	2·9546	1·8093	2·0892
0·3	2·9503	2·9503	2·9503	1·8066	2·0862
0·4	2·9486	2·9486	2·9486	1·8056	2·0850
0·5	2·9475	2·9475	2·9475	1·8049	2·0842

Table 3. X-ray intensity calculation for $Co_{1+y}Sn_yFe_{2-2y-x}Cr_xO_4$ ($y = 0{\cdot}05$) system.

	I_{220}/I_{440}		I_{400}/I_{440}		Amount of Fe^{3+} in octahedral site	Fe^{3+} tetra.
x	Obs.	Cal.	Obs.	Cal.		Fe^{3+} octa.
0·0	0·586	0·600	0·659	0·512	0·94	1·021
0·1	0·529	0·589	0·376	0·497	0·88	1·045
0·2	0·451	0·602	0·441	0·497	0·82	1·073
0·3	0·545	0·613	0·545	0·499	0·76	1·105
0·4	0·451	0·610	0·492	0·494	0·70	1·143
0·5	0·415	0·624	0·629	0·495	0·64	1·187

Table 4. Cation distribution, s_s and n_B for $Co_{1+y}Sn_yFe_{2-2y-x}Cr_xO_4$ ($y = 0{\cdot}05$) system.

			n_B (μ_B)	
x	Cation distribution	s_s (emu/g)	Obs.	Cal.
0·1	$(Fe_{0.92}Co_{0.08})^A$ $[Fe_{0.88}Sn_{0.05}Co_{0.97}Cr_{0.1}]^B$	65·83	2·80	2·77
0·2	$(Fe_{0.88}Co_{0.12})^A$ $[Fe_{0.82}Sn_{0.05}Co_{0.93}Cr_{0.2}]^B$	64·52	2·74	2·73
0·3	$(Fe_{0.84}Co_{0.16})^A$ $[Fe_{0.76}Sn_{0.05}Co_{0.89}Cr_{0.3}]^B$	63·21	2·68	2·69
0·4	$(Fe_{0.80}Co_{0.20})^A$ $[Fe_{0.70}Sn_{0.05}Co_{0.85}Cr_{0.4}]^B$	61·42	2·60	2·65
0·5	$(Fe_{0.76}Co_{0.24})^A$ $[Fe_{0.64}Sn_{0.05}Co_{0.81}Cr_{0.5}]^B$	60·11	2·54	2·61

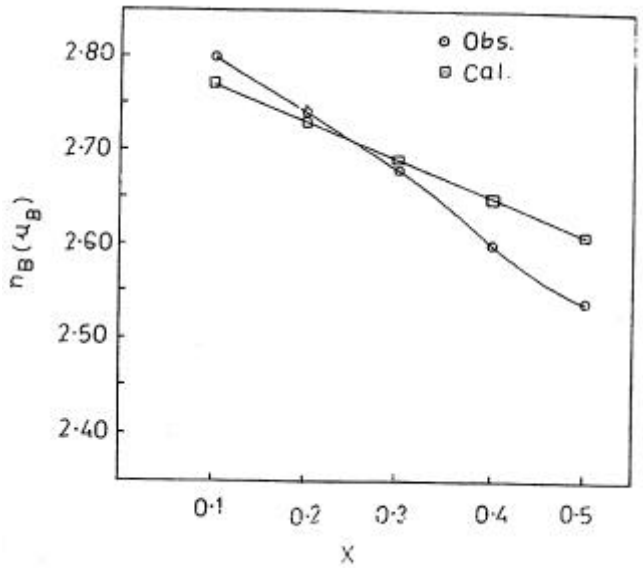

Figure 3. Variation of n_B (μ_B) with Cr^{3+} concentration, x.

$$n_B^N = M_B(x) - M_A(x), \quad (5)$$

where, M_B and M_A are the B and A sublattice magnetic moments in μ_B. The $n_B^N(\mu_B)$ values for the present system were calculated using the ionic magnetic moments of Fe^{3+}, Co^{2+}, Cr^{3+} and Sn^{4+} with their respective values $5\mu_B$, $3\mu_B$, $3\mu_B$ and $0\mu_B$. These $n_B^N(\mu_B)$ values for $x = 0{\cdot}1$ to $0{\cdot}5$ are in good agreement with the observed n_B values.

Typical plots of relative low field a.c. susceptibility, c_T/c_{RT} (RT = room temperature), against temperature, T, for typical samples with $x = 0$, $0{\cdot}1$ and $0{\cdot}2$ are shown in figure 4, which exhibit normal ferrimagnetic behaviour. The Curie temperature, T_C, determined from a.c. susceptibility measurements is depicted in figure 5, as a function of chromium content, x. According to Neel's model, the A–B interaction is most dominant in ferrites, therefore, Curie temperature of the ferrites are determined from the overall strength of A–B interaction (Neel 1950). The strength of A–B interaction is a function of the number of $Fe_A^{3+} - O^{2-} - Fe_B^{3+}$ linkage (Gilleo 1960), which in turn depends upon the number of Fe^{3+} ions in the formula unit and their distribution amongst tetrahedral (A) and octahedral [B] sites. In the present system of ferrite, it is observed that Cr^{3+} ions ($3\mu_B$) replace Fe^{3+} ions ($5\mu_B$) on the octahedral B site. This results in decreasing the strength of A–B exchange interactions which leads to decrease in Curie temperature as observed experimentally (figure 5).

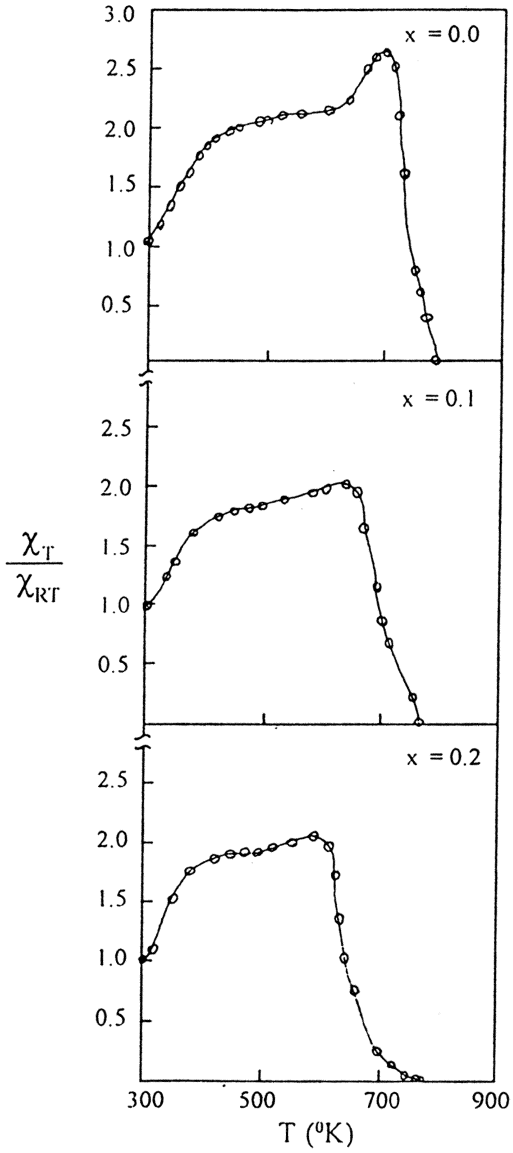

Figure 4. Plots of normalized a.c. susceptibility c_T/c_{RT} against temperature (x = 0·0, 0·1 and 0·2).

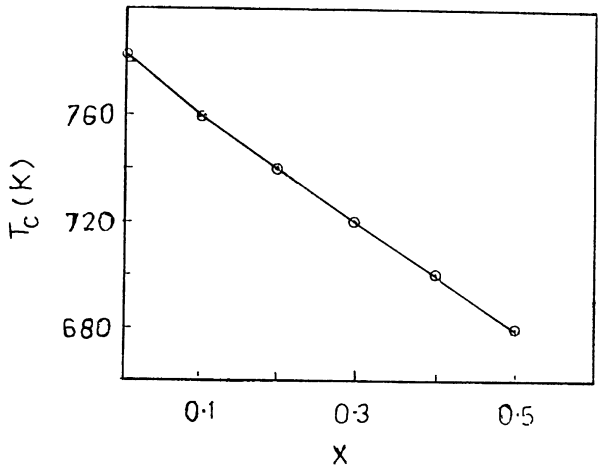

Figure 5. Variation of Curie temperature (T_C) with Cr^{3+} concentration, x.

4. Conclusions

The lattice parameter increases up to $x = 0{\cdot}2$ and then starts decreasing for $x > 0{\cdot}2$. The structure is found to be collinear for all values of x studied. The cation distribution obtained from X-ray intensity calculation and magnetization are in good agreement. The Neel temperature decreases with increase in x. Addition of chromium in presence of Sn^{4+} decreases the saturation magnetization and thereby decreases the Curie temperature.

Acknowledgements

One of the authors (AAP) is thankful to UGC, New Delhi, for providing a Teacher's Fellowship under FDP. (KMJ) is thankful to UGC, New Delhi, for granting the major research project. Authors are also thankful to USIC, Shivaji University, Kolhapur, for providing X-ray diffraction patterns.

References

Blasse G 1964 *Philips Res. Rep. Suppl.* 3

Bradley F N 1971 *Materials for magnetic functions* (New York: Hayden) p. 78

Buerger M G 1960 *Crystal structure analysis* (New York: Wiley)

Cullity B D 1959 *Elements of X-ray diffraction* (Reading, Mass: Addison Wesley)

Furuhashi H, Inagari M and Naka S 1973 *J. Inorg. Nuclear Chem.* **35** 3009

Gilleo M A 1960 *J. Phys. Chem. Solids* **13** 33

Goodenough J B and Loeb A L 1953 *Phys. Rev.* **98** 391

Joshi H H, Jotania R B and Kulkarni R G 1993 *Asian J. Phys.* **2** 88

Khan D C, Mishra M and Das A R 1982 *J. Appl. Phys.* **53** 2722

Kwang Pyo Chae, Young Bae Lee, Jae Gwang Lee and Sung Ho Lee 2000 *J. Magn. & Magn. Mater.* **220** 59

Neel L 1950 *C.R. Acad. Sci., Paris* **230** 375

Nogues J, Phig T, Jotania R B, Upadyay R V, Kulkarni R G and Rao K V 1991 *J. Magn. & Magn. Mater.* **99** 275

Ohinishi H and Teranishi T 1961 *J. Phys. Soc. Jpn* **16** 36

Otero Arean C, Rodriguez Blanco J L, Rubio Gonzalez J M and Trobajoa Fermandez M C 1990 *J. Mater. Sci. Lett.* **9** 229

Porta P, Stone F S and Turner R G 1974 *J. Solid State Chem.* **11** 135

Radhakrishnamurty C, Likhite S D and Shastry P 1971 *Philos. Mag.* **23** 503

Radhakrishnamurty C, Likhite S D and Sahasrabudhe P 1978 *Proc. Indian Acad. Sci.* (*Chem. Sci.*) **A87** 245

Sawataky G A, Van der Wouds F and Morrish A H 1968 *J. Appl. Phys.* **39** 1204

Shinde S S, Jadhav K M, Bichile G K, Trivedi Bimal S and Kulkarni R G 1998 *Bull. Mater. Sci.* **21** 409